PHYSICAL REVIEW B **85**, 144525 (2012)

Local density of states in metal-topological superconductor hybrid systems

Marco Gibertini,[1,*] Fabio Taddei,[2] Marco Polini,[2] and Rosario Fazio[1,†]
[1]*NEST, Scuola Normale Superiore and Istituto Nanoscienze-CNR, I-56126 Pisa, Italy*
[2]*NEST, Istituto Nanoscienze-CNR and Scuola Normale Superiore, I-56126 Pisa, Italy*
(Received 29 November 2011; revised manuscript received 24 February 2012; published 30 April 2012)

We study by means of the recursive Green's function technique the local density of states of (finite and

continuum-model Hamiltonian[13,14,20] reads[16]

$$\begin{aligned}\hat{\mathcal{H}}_{\rm RZ} &= \sum_{i,j}[h_{\rm RZ}(i,j)]_{\sigma\sigma'}\hat{c}^\dagger_{i,\sigma}\hat{c}_{j,\sigma'}\\ &= -t\sum_{\langle i,j\rangle,\sigma}\hat{c}^\dagger_{i,\sigma}\hat{c}_{j,\sigma}+(\varepsilon_0-\mu)\sum_{i,\sigma}\hat{c}^\dagger_{i,\sigma}\hat{c}_{i,\sigma}\\ &\quad+i\alpha\sum_{\langle i,j\rangle,\sigma,\sigma'}\left(\nu'_{ij}\sigma^x_{\sigma\sigma'}-\nu_{ij}\sigma^y_{\sigma\sigma'}\right)\hat{c}^\dagger_{i,\sigma}\hat{c}_{j,\sigma'}\\ &\quad+V\sum_{i,\sigma,\sigma'}\sigma^x_{\sigma\sigma'}\hat{c}^\dagger_{i,\sigma}\hat{c}_{i,\sigma'}. \end{aligned}\tag{1}$$

Here $\varepsilon_0=4t$ is a uniform on-site energy which sets the zero of energy, σ^i are spin-$\frac{1}{2}$ Pauli matrices, $\nu_{ij}=\hat{\boldsymbol{x}}\cdot\hat{\boldsymbol{d}}_{ij}$ and $\nu'_{ij}=\hat{\boldsymbol{y}}\cdot\hat{\boldsymbol{d}}_{ij}$, with $\hat{\boldsymbol{d}}_{ij}=(\boldsymbol{r}_i-\boldsymbol{r}_j)/|\boldsymbol{r}_i-\boldsymbol{r}_j|$ being the unit vector connecting site j to site i.

If we now allow sections of the nanowire to be in contact with a bulk s-wave superconductor, the proximity effect induces a nonvanishing superconducting pairing in these sections so that the complete Hamiltonian becomes

$$\hat{\mathcal{H}}=\hat{\mathcal{H}}_{\rm RZ}+\hat{\mathcal{H}}_{\rm S},\tag{2}$$

where

$$\hat{\mathcal{H}}_{\rm S}=\sum_i[\Delta(i)\hat{c}^\dagger_{i,\uparrow}\hat{c}^\dagger_{i,\downarrow}+{\rm H.c.}].\tag{3}$$

For simplicity we assume $\Delta(i)$ to be piecewise constant, with $|\Delta(i)|=\Delta$ in the regions in contact with the superconductor and $\Delta(i)=0$ otherwise. Moreover, we assume that a barrier is present at the boundary between proximized and nonproximized sections, leading to a decrease of the value of the hopping energy t and of the SO coupling α by the same factor γ.[21]

Finally, it is convenient to introduce the Nambu spinors $\hat{\Psi}_i=(\hat{c}_{i,\uparrow},\hat{c}_{i,\downarrow},\hat{c}^\dagger_{i,\downarrow},-\hat{c}^\dagger_{i,\uparrow})^T$ and rewrite the Hamiltonian (2) in the form

$$\hat{\mathcal{H}}=\frac{1}{2}\sum_{i,j}\hat{\Psi}^\dagger_i\mathcal{H}_{\rm BdG}(i,j)\hat{\Psi}_j,\tag{4}$$

where

$$\mathcal{H}_{\rm BdG}(i,j)=\begin{pmatrix}h_{\rm RZ}(i,j) & \Delta(i)\delta_{ij}\\ \Delta(i)\delta_{ij} & -\sigma^y h^*_{\rm RZ}(i,j)\sigma^y\end{pmatrix}\tag{5}$$

is the Bogoliubov-de Gennes (BdG) Hamiltonian.[22]

The tight-binding Hamiltonian (5) will be the starting point of our analysis.

A. Phase diagram

Before proceeding with the study of the LDOS we need to know in which regions of parameter space we should expect Majorana fermions. This problem has been addressed in Refs. 13 and 14 in the strictly one-dimensional case and in the continuum limit ($a\to 0$): The S-nanowire is in the topological phase when $|V|>\sqrt{\mu^2+\Delta^2}$, while it is in the trivial phase otherwise. Thus, the phase boundary occurs along the line implicitly defined by

$$V^2=\mu^2+\Delta^2.\tag{6}$$

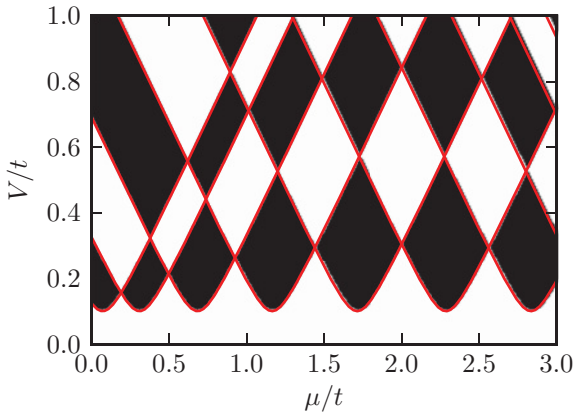

FIG. 1. (Color online) Phase diagram of an infinite superconducting wire as a function of the chemical potential μ and the Zeeman field V. White regions correspond to a trivial system ($\mathcal{Q}=+1$), while dark regions identify the topologically nontrivial phase ($\mathcal{Q}=-1$). Red thick lines illustrate the prediction in Eq. (8) for the phase boundaries. These results refer to the following set of parameters: $W/a=10$, $\alpha/t=0.1$, and $\Delta/t=0.1$.

The phase diagram of multiband ($W/a\neq 1$) nanowires has been investigated numerically in Refs. 17 and 20. The phase of a uniform system can be determined, for instance, from the evaluation of the following Pfaffian formula[23] for the topological invariant

$$\mathcal{Q}={\rm sign}\{{\rm Pf}[\mathcal{H}_{\rm BdG}(0)\sigma^y\tau^y]{\rm Pf}[\mathcal{H}_{\rm BdG}(\pi/a)\sigma^y\tau^y]\},\tag{7}$$

where $\mathcal{H}_{\rm BdG}(k_x)$ is the Fourier transform of the BdG Hamiltonian in Eq. (5), while τ^i are Pauli matrices acting on the particle-hole degrees of freedom. In Fig. 1 we report numerical results for a given system ($W/a=10$, $\alpha/t=0.1$, and $\Delta/t=0.1$) as a function of the chemical potential μ and Zeeman field V, obtained using an algorithm developed by Wimmer.[24] The topologically trivial phase corresponds to $\mathcal{Q}=+1$ (white regions), while the nontrivial one is signaled by $\mathcal{Q}=-1$ (dark regions). The phase boundaries in this figure (red thick lines) have been derived analytically and are given by the following result:

$$(\mu-\varepsilon_0-\varepsilon_\lambda\pm 2t)^2+\Delta^2=V^2.\tag{8}$$

Here $\varepsilon_0+\varepsilon_\lambda\mp 2t$ are the eigenenergies of $\mathcal{H}_{\rm BdG}(k)$ for $k=0,\pi/a$, respectively, when $V=\Delta=\mu=0$. The following expression holds for the energies ε_λ

$$\varepsilon_\lambda=-2\sqrt{t^2+\alpha^2}\cos\left(\frac{\lambda\pi}{n+1}\right);\quad \lambda=1,\ldots,n=W/a.\tag{9}$$

A thorough derivation of Eqs. (8) and (9) is given in Appendix A.

III. LDOS: NUMERICAL RESULTS

As we mentioned in the Introduction, the LDOS can be accessed in experiments using scanning tunneling microscopy (STM). The STM experimental setup is sketched in Fig. 2. When the metallic tip of the STM is moved close to the nanowire a tunneling current can flow. By locally measuring this current I as a function of the tip-sample bias voltage V, the

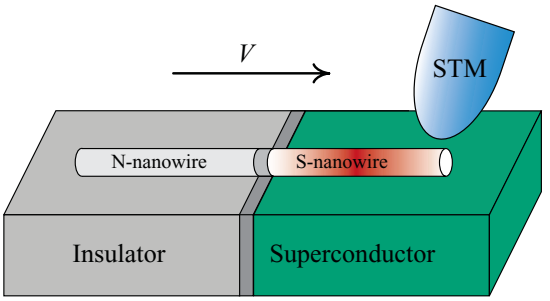

FIG. 2. (Color online) Experimental setup adopted in measurements of the LDOS of a nanowire (in this case comprising a normal electrode and a superconducting segment separated by a barrier). The differential conductance obtained from the current between the tip of the scanning tunneling microscope (STM) and the nanowire is proportional to the LDOS of the nanowire according to Eq. (10).

LDOS at a given position $\boldsymbol{r}$ and energy E can be reconstructed from the differential conductance at $eV = E$:[25,26]

$$\frac{dI}{dV}(\boldsymbol{r},eV) \propto \mathcal{N}(\boldsymbol{r},E = eV). \tag{10}$$

As a consequence, it is particularly interesting to investigate the LDOS theoretically and make predictions that can be tested in experiments.

In what follows the LDOS is computed through the standard relation

$$\mathcal{N}(\boldsymbol{r},E) = -\frac{1}{2\pi}\Im m\{\mathrm{Tr}[G(\boldsymbol{r},E)]\}, \tag{11}$$

where $G(\boldsymbol{r},E)$ is the Green's function and the factor 2 in the denominator is introduced to avoid a double counting of particle and hole degrees-of-freedom intrinsic in the BdG formalism. We have computed $G(\boldsymbol{r},E)$ using a recursive Green's function technique similar to the one adopted in Ref. 17, suitably generalized to include the effects of semi-infinite leads.[27] For simplicity, in the following we fix the width $W = 10a$, the SO coupling strength $\alpha = 0.1t$, and the superconducting pairing $\Delta = 0.1t$.

A. Isolated S-nanowire

Let us first consider an isolated S-nanowire of finite length ($L = 100a$). This situation has been addressed before[17,18] and it is considered here for the sake of reference. We consider two cases: (i) $\mu = 0$ and $V/t = 0.2$ (with one open channel in the absence of superconducting pairing) and (ii) $\mu = 0$ and $V/t = 0.6$ (with two open channels). According to Fig. 1, in case (i) the wire is topologically nontrivial, while in case (ii) the wire is topologically trivial. For case (i), Fig. 3(a) shows that the LDOS at an energy close to the chemical potential is characterized by the presence of bound states at both ends of the wire. The presence of Majorana bound states appears as a sharp peak at zero energy in the LDOS as a function of energy at a given position in space [see Fig. 3(b)]. According to Fig. 3(c), these Majorana bound states have oscillating wave functions which decay exponentially inside the bulk of the S-nanowire with a typical length scale (effective superconducting coherence length) $\xi \approx 10a$.

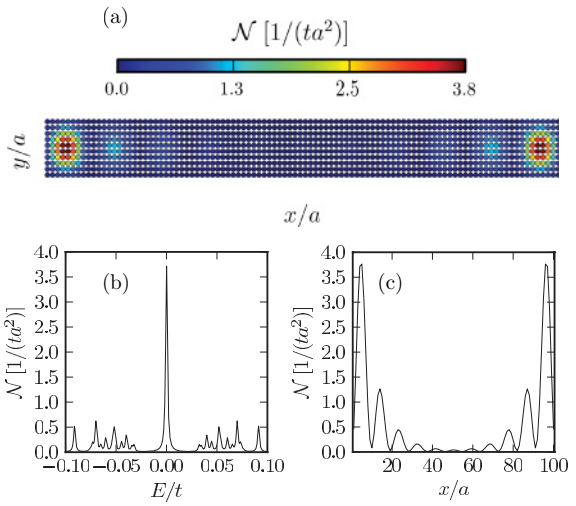

FIG. 3. (Color online) (a) LDOS of an isolated superconducting nanowire in the topologically nontrivial phase ($\mu/t = 0$, $V/t = 0.2$) at an energy very close to the chemical potential ($E \simeq 0$). Bound states at both ends of the wire are apparent. (b) LDOS at a given position ($x/a = 4$, $y/a = 5$) as a function of energy. A sharp peak corresponding to a Majorana bound state is present at $E = 0$. (c) LDOS at $E \simeq 0$ as a function of x along the middle of the wire ($y/a = 5$).

On the contrary, in case (ii) where the wire is topologically trivial (and presents two transverse channels in the absence of superconducting pairing) the LDOS at the chemical-potential energy is almost zero throughout the wire, while it shows spatial features only at finite energies [see Fig. 4(a) for $E/t \simeq \pm 0.002$, where E is measured from the chemical potential]. In particular, as shown in Fig. 4(c), the LDOS oscillates and decreases moving toward the center of the wire, the length scale of the exponential drop, $\xi \approx 30a$, being much larger

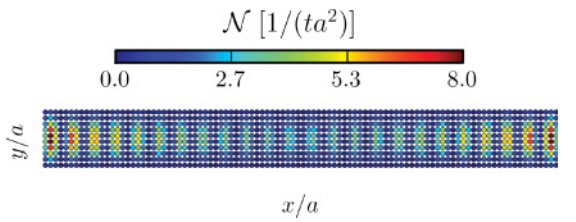

than for case (i). Now, if the two channels were decoupled, two Majorana modes would have appeared at each end of the wire, one for each open channel. However, since the two transverse channels are actually coupled in the wire, a single fermion at each end appears at a finite energy,[17] as though coming from the hybridization of the two Majorana modes. Figure 4(b) shows one pair of peaks at $E/t \simeq \pm 0.002$ and another pair (with smaller amplitude) at $E/t \simeq \pm 0.007$. The presence of two pairs of peaks is due to the long coherence length which allows the two localized fermions at the ends of the wire to strongly hybridize, lifting the parity degeneracy of the system. We have checked that for a longer wire ($L/a = 400$) the overlap between the fermions vanishes and the two peaks at $E/t \simeq 0.002$ and $E/t \simeq 0.007$ merge into a single double-degenerate peak at energy $E/t \simeq 0.001$. The latter energy depends on the width of the nanowire.[28]

B. S-nanowire attached to a normal electrode

In this section we analyze the impact of a normal lead attached to the S-nanowire. This situation can arise, for instance, when the nanowire is only partially in proximity to a bulk superconductor so that part of the nanowire is in the normal state (as shown in Fig. 2). In order to get rid of finite-size effects, we consider a semi-infinite S-nanowire coupled to a normal lead. The case of a finite-length S-nanowire coupled to two normal leads at both ends does not yield additional significant information.

In Fig. 5 we plot the LDOS, at different positions, as a function of energy for several values of the barrier strength

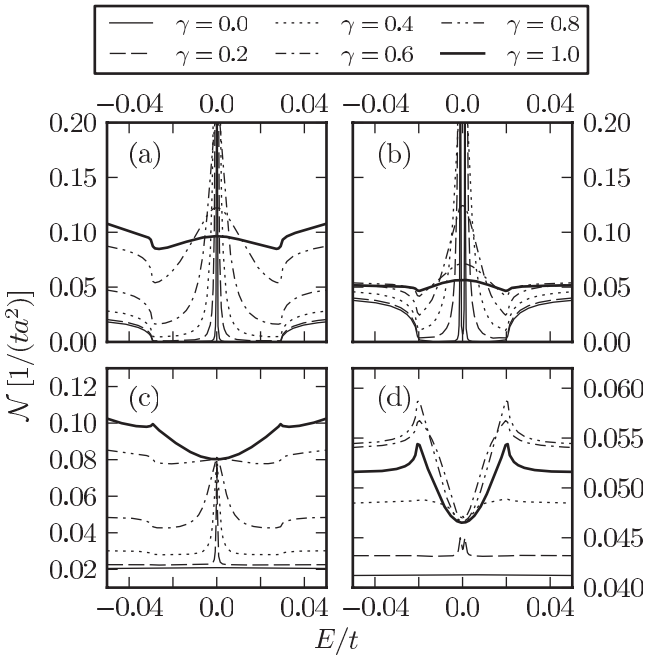

FIG. 5. LDOS of a superconducting nanowire coupled to a normal lead as a function of energy, at fixed positions in space, in the nontrivial [$\mu/t = 0$ and $V/t = 0.2$, panels (a) and (c)], and trivial [$\mu/t = 0$, $V/t = 0.6$, panels (b) and (d)] phase. Panels (a) and (b) refer to a position just inside the superconducting part ($x/a = 51$), while panels (c) and (d) refer to a position just inside the normal part of the junction ($x/a = 50$). The interface is at $x/a = 50.5$.

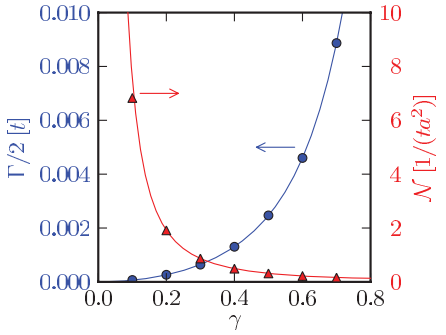

FIG. 6. (Color online) Fitted values [through Eq. (12)] of the half width at half maximum $\Gamma/2$ (blue circles) and height at zero energy $\mathcal{N}$ (red triangles) of the peak in the LDOS at a position just inside the superconducting nanowire in the nontrivial phase. Solid lines are just guides for the eye.

γ. The two plots on the left [(a) and (c)] are for a nontrivial nanowire with $\mu/t = 0$ and $V/t = 0.2$, while the two plots on the right [(b) and (d)] refer to a topologically trivial nanowire with $\mu/t = 0$ and $V/t = 0.6$. Moreover, the top panels [(a) and (b)] refer to a position close to the interface in the S-nanowire, while the bottom panels [(c) and (d)] to a position close to the interface in the normal lead. When γ is small the LDOS in the S-nanowire presents a finite gap E_g which is just a fraction of the superconducting pairing Δ owing to the presence of the Zeeman field. Namely, $E_g \simeq 0.03t = 0.3\Delta$ for the nontrivial nanowire and $E_g \simeq 0.018t = 0.18\Delta$ for the trivial case. Within the gap, Fig. 5(a) shows a sharp Majorana peak at zero energy which broadens as γ increases[29,30] and eventually disappears when $\gamma \to 1$. Such a peak can be fitted with the following Lorentzian function:

$$\mathcal{N}(\boldsymbol{r}, E) \simeq \mathcal{N} \frac{(\Gamma/2)^2}{E^2 + (\Gamma/2)^2}, \tag{12}$$

where $\Gamma/2$ is the half width at half maximum and $\mathcal{N}$ is the height at zero energy. The result of the fit is reported in Fig. 6: $\Gamma/2$ and $\mathcal{N}$ are plotted as functions of γ. Remarkably, $\Gamma/2$ depends only very weakly on the position in the S-nanowire where the LDOS is calculated.

Interestingly, the Majorana peak is present also in the LDOS of the normal lead [Fig. 5(c)] as long as γ is not exactly zero: The peak is still clearly distinguishable up to $\gamma \simeq 0.6$. Moreover, singularities develop at energies corresponding to $\pm E_g$ as γ tends to 1.

In the trivial phase, the LDOS in the S-nanowire at a position close to the interface [Fig. 5(b)] presents a single pair of peaks at $\gamma = 0$ (as compared to Fig. 4), since, being semi-infinite, the ends of the S-nanowire are sufficiently far away to be decoupled. Such peaks quickly broaden as γ increases and eventually merge into a single peak at $\gamma \simeq 0.3$ (a further increase of γ leads to the disappearing of the peak). As a result, as long as the coupling between the S-nanowire and the normal lead is not too strong, nontrivial and trivial phases can be distinguished from a measurement of the LDOS in the S-nanowire given a sufficiently large energy resolution (in the present case higher than 1% of the pairing Δ). On the contrary, only a very weak double-peak structure is visible in

the LDOS in the normal lead at a position close to the interface and for small values of γ [see Figs. 5(d)].

We mention that important clues on the topological phase of a S-nanowire coupled to a normal electrode can be also retrieved using a different transport setup with respect to the one depicted in Fig. 2. Indeed, instead of considering the current from the STM tip to the sample, it would, in principle, be possible to study directly transport through the NS junction present in the nanowire. Even though a theoretical analysis of this configuration is beyond the scope of the present work, in Appendix B we report on the low-bias conductance of the NS junction. We find that, in the tunneling limit, the approximate quantization of the conductance can be exploited to identify the topological phase of the nanowire.[29,31,32] We also remark that, even for transparent barriers, clear signatures of the presence of Majorana fermions can be extracted from the transport properties of the NS junction provided that a quantum point contact is present close to the interface.[33]

Let us now analyze how the LDOS changes when the S-nanowire is driven through a topological phase transition.[34] In Fig. 7(a) we plot the topological invariant $\mathcal{Q}$ [calculated using Eq. (7)] and the number of open channels ($N_{\rm oc}$) as functions of the chemical potential μ for a fixed Zeeman field $V = 0.3t$. The S-nanowire goes through a transition, from the nontrivial ($\mathcal{Q} = -1$) to the trivial ($\mathcal{Q} = +1$) phase, at $\mu \simeq 0.026t$. Interestingly, the number of channels increases from 1 to 2 at a much smaller value of the chemical potential

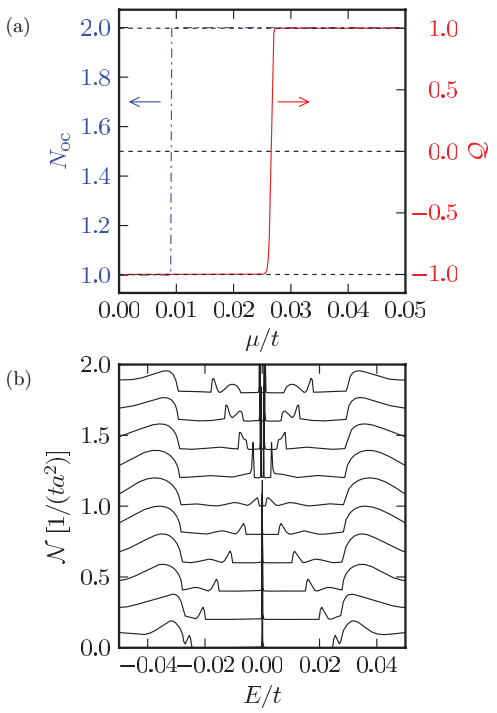

FIG. 7. (Color online) (a) Topological invariant $\mathcal{Q}$ (red solid line) and number of open transverse channels $N_{\rm oc}$ (blue dash-dotted line) as functions of the chemical potential μ for a system with $V/t = 0.3$. A phase transition occurs at $\mu/t \simeq 0.026$. (b) LDOS at a position inside a semi-infinite superconducting nanowire for different values of the chemical potential μ keeping $V/t = 0.3$ fixed. Results have been offset vertically for clarity, with an increasing value of the chemical potential from bottom ($\mu/t = 0$) to top ($\mu/t = 0.05$).

$\mu \simeq 0.01t$ such that the nontrivial phase persists even in the presence of two open channels. This observation is in apparent contradiction with the intuitive picture adopted in the literature to explain the phase diagram of superconducting nanowires, that is, that a pair of Majorana fermions at the ends of the wire is associated with each open channel and that pairs of Majorana fermions on the same end can couple and form complex (Dirac) fermions. Accordingly, there should be a single isolated Majorana fermion at each end of the nanowire whenever the number of open channels is odd. On the other hand, this intuitive picture should be treated with care, simply because one concept (presence of Majorana fermions) is related to a superconducting wire while the other (number of open channels) to a normal one. Indeed, already in Ref. 17 it was noticed that the system can be in the topologically trivial phase even when $N_{\rm oc}$ is odd. Here, we are observing the complementary situation in which the topological phase persists when $N_{\rm oc}$ is even. We believe that the underlying explanation is the same for both cases: the failure of the intuitive picture reported above to explain the whole phase diagram. As a consequence, we remark that the topological invariant is not necessarily in a one-to-one correspondence with the parity of the number of open channels. In Fig. 7(b) the LDOS as a function of energy is shown at a position inside the S-nanowire ($x = 50a$, measured from the interface, and $y = W/2 = 5a$) when γ is close to zero. Different curves correspond to different values of the chemical potential, with a vertical offset proportional to μ. The Majorana peak splits into two Dirac-fermion peaks at finite energy as the chemical potential moves through the phase transition. Besides, we also observe that the effective gap $E_{\rm g}$ initially decreases for increasing μ, then vanishes at the phase transition, and thereafter increases again. Similar results (concerning the differential tunneling conductance at one end of a nanowire) have been recently presented in Ref. 18.

C. SNS structure

Let us now consider two semi-infinite S-nanowires connected through a normal nanowire (N nanowire). For simplicity we assume transparent barriers at the interfaces and we set

$$\Delta(i) \equiv \Delta(x/a) = \begin{cases} \Delta e^{i\varphi_{\rm L}} & x < -L/2, \\ 0 & |x| \leqslant L/2, \\ \Delta e^{i\varphi_{\rm R}} & x > L/2; \end{cases} \tag{13}$$

that is, we allow for a finite phase difference $\Delta\varphi = \varphi_{\rm R} - \varphi_{\rm L}$ between the superconducting paring in the right and left S-nanowires, L being the length of the N nanowire. Independently of the topological phase of the system, Andreev bound states (ABSs) appear as sharp peaks in the LDOS (see Fig. 8) and the ABS spectrum can thus be reconstructed from the energies at which such peaks occur. As we discuss at length below, what differs between topologically trivial and nontrivial phases is the parity of the number of zero-energy crossings in the ABS spectrum, which is related to the presence or absence of such a crossing at $\Delta\varphi = \pi$ (protected by fermion parity). This result is in agreement with similar calculations performed for a strictly one-dimensional system,[13,35] for a

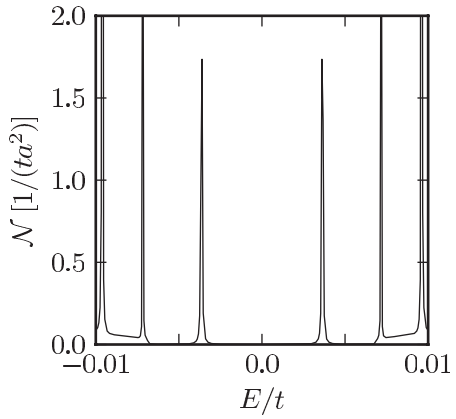

FIG. 8. LDOS as a function of energy at a given position close to the interface inside the left superconducting nanowire. Sharp peaks corresponding to Andreev bound states appear both within the effective gap E_g ($\simeq 0.007t$) and inside the continuum. These results refer to the following set of parameters: $\Delta\varphi = 2.0$, $\mu/t = 0$, $V/t = 0.8$, and $L/a = 0$.

two-dimensional SNS junction,[36] and for a quantum spin-Hall insulator sandwiched between superconducting leads.[37]

We start by considering the short-junction limit, $L \ll \xi$ (where $\xi \propto ta/E_g$ is the effective superconducting coherence length), in which we have a single ABS for each open channel. $L = 0$ is a particular case in which the N nanowire is absent and we have a steplike jump from φ_L to φ_R in the phase of a S-nanowire. In Fig. 9 we show, for $L = 0$, the ABS energies as a function of $\Delta\varphi$ for a topologically nontrivial [panel (a) for $\mu/t = 0$ and $V/t = 0.2$] and trivial [panel (b) for $\mu/t = 0.15$ and $V/t = 0.1$] S-nanowires. In both cases we have a single ABS (with its opposite energy counterpart). The main difference between the two cases is that the number of zero-energy crossings is odd in the nontrivial phase while it is even in the trivial case, in agreement with Ref. 13. Furthermore, even though the overall periodicity of the ABS spectrum is 2π in both cases, the periodicity of a single branch of the ABS spectrum is 4π only for the nontrivial situation. In particular, the change of $\Delta\varphi$ by 2π at a fixed energy leads to the swapping of an ABS with its charge-conjugate state which has opposite fermion parity. In terms of Josephson current this leads to the fractional Josephson effect[9] and can be interpreted either as a 4π periodicity or as a two-valuedness of the Josephson current. For simplicity in the following we will address the topologically nontrivial ABS spectrum as 4π periodic.

It is now interesting to compare the plot in Fig. 9(a) with the ABS spectrum relative to a short, one-dimensional, SNS Josephson junction with $p_x + ip_y$ superconducting order parameter. An expression for the latter has been obtained, under the Andreev approximation (which assumes an order parameter much smaller than the Fermi energy), in Ref. 38:

$$E_{abs} = \pm\Delta_{abs}\sqrt{\mathcal{T}}\cos(\Delta\varphi/2), \tag{14}$$

where $\mathcal{T}$ is the transmission probability of the N region and Δ_{abs} is an effective order parameter for the ABS. The solid line in Fig. 9(a) shows the result of a best fit, with respect to Δ_{abs}, once $\mathcal{T}$ is set to 1. The agreement between the numerical results (red open circles) and the fit is quite

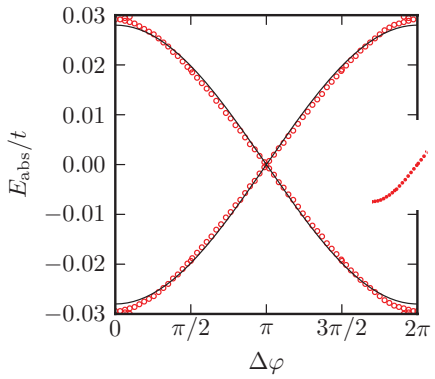

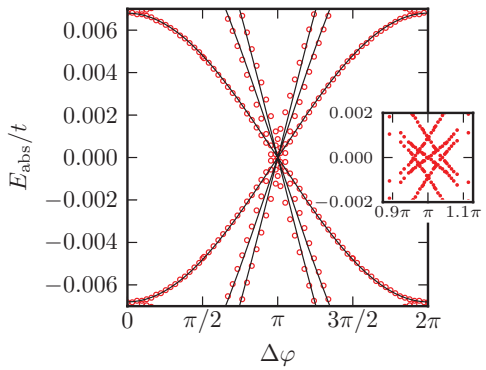
0.006
0.004
0.002
0.000
−0.002
−0.004
−0.006
$E_{\rm abs}/t$
0
$\pi/2$
π
$3\pi/2$
2π
$\Delta\varphi$
0.002
0.000
−0.002
0.9π
π
1.1π

(a)

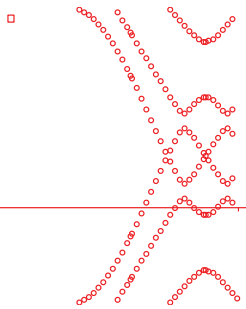


0.03

values of such parameters, the nanowire presents a nontrivial topological phase in which a pair of Majorana modes, at an energy equal to the chemical potential, are localized at its ends. We have first derived an analytic expression for the phase boundaries of an infinitely long multiband nanowire. We have then numerically calculated and analyzed the local density of states of such nanowires in the case when they are coupled to normal regions (such as electrodes or links) and we have compared the topologically nontrivial and trivial phases in different situations. When the nanowire is coupled to a normal electrode we have found that the peak in the local density of states at zero energy (with respect to the chemical potential), corresponding to the Majorana mode, broadens with increasing coupling strength to the electrode, eventually disappearing for a transparent interface. Interestingly, for finite coupling the peak is also present in the normal electrode, though being of smaller amplitude and broadening more rapidly with the strength of the coupling. In the trivial phase, and when the nanowire possesses two open channels in the absence of superconducting pairing, a pair of peaks at finite energies appears as due to the hybridization of the two Majorana modes that would exist if the two channels of the nanowire were not coupled. Such peaks broaden with increasing coupling strength to the normal electrode, eventually merging for sufficiently large coupling. In the normal electrode only weak features survive. From the analysis of the topological phase transition, driven by varying the chemical potential at fixed Zeeman field, we have found that the nanowire remains in the topologically nontrivial phase even after the number of open channels goes from one to two. This suggests that, contrary to the intuitive picture often referred to in the literature, the one-to-one correspondence between the topological invariant and the parity of the number of open channels is only approximate and should be treated with care. We have then considered the situation in which two semi-infinite nanowires (kept at different superconducting phases) are connected through a normal link of length L. Independently of the topological phase the density of states presents peaks due to Andreev bound states whose position in energy depends on the superconducting phase difference $\Delta\varphi$. While in the trivial phase the number of zero-energy crossings is even, in the topologically nontrivial phase this number is odd owing to the presence of a fermion-parity-protected crossing at $\Delta\varphi = \pi$. This difference in the parity of the number of zero-energy crossings reflects the presence of at least one branch of Andreev-bound-state energy which is 4π periodic (instead of the usual 2π periodicity), leading to the so-called fractional Josephson effect. This anomalous 4π periodicity of the Josephson current has been usually introduced in strictly one-dimensional systems while we have checked that it survives also in a multiband nanowire, in agreement with Ref. 41.

ACKNOWLEDGMENTS

We would like to acknowledge fruitful discussions with C.W.J. Beenakker and D. Rainis. This work has been supported by the EU FP7 Programme under Grant Agreements No. 234970-NANOCTM, No. 248629-SOLID, No. 233992-QNEMS, No. 238345-GEOMDISS, and No. 215368-SEMISPINNET.

APPENDIX A: DERIVATION OF THE PHASE DIAGRAM

We first need to determine the eigenvalues and eigenvectors of $\mathcal{H}_{\rm BdG}(k_x)$ for $k_x = 0$ and π/a, when $V = \Delta = 0$. The difference between $k_x = 0,\pi/a$ is just a shift $\pm 2t$ in the chemical potential; that is,

$$\mathcal{H}_{\rm BdG}(k_x = 0,\pi/a) = \mathcal{H}_0 + [\varepsilon_0 - (\mu \pm 2t)]\tau_z. \quad \text{(A1)}$$

Moreover, we are assuming $\Delta = 0$, so that

$$\mathcal{H}_0 = \begin{pmatrix} \mathcal{H}_{\rm p} & 0 \\ 0 & -\sigma^y \mathcal{H}_{\rm p}^* \sigma^y \end{pmatrix}. \quad \text{(A2)}$$

Thus, it suffices to consider the particle Hamiltonian $\mathcal{H}_{\rm p}$. For a wire of width $W/a = n$ the characteristic polynomial $L_n(\varepsilon;\alpha)$ of $\mathcal{H}_{\rm p}$ can be defined recursively as

$$L_n(\varepsilon;\alpha) = \varepsilon L_{n-1}(\varepsilon;\alpha) - (t^2 + \alpha^2) L_{n-2}(\varepsilon;\alpha), \quad \text{(A3)}$$

with $L_0(\varepsilon;\alpha) = 1$ and $L_1(\varepsilon;\alpha) = \varepsilon$. A formal solution to the recursive relation (A3)

is not diagonal, it is still useful to introduce it. Indeed, we can then write

$$\mathcal{H}_{\rm BdG}(k_x)\sigma^y\tau^y = U_{\rm BdG}\mathcal{D}(k_x)(\sigma^y\tau^y U_{\rm BdG})^\dagger \quad \text{(A11)}$$

and, since by particle-hole symmetry we have that

$$\sigma^y\tau^y U_{\rm BdG} = U^*_{\rm BdG}\tau^x, \quad \text{(A12)}$$

the Pfaffian can be written as

$$\begin{aligned}\mathrm{Pf}[\mathcal{H}_{\rm BdG}(k_x)\sigma^y\tau^y] &= \mathrm{Pf}\left[U_{\rm BdG}\mathcal{D}(k_x)\tau^x U^T_{\rm BdG}\right] \\ &= \det(U_{\rm BdG})\mathrm{Pf}[\mathcal{D}(k_x)\tau^x] \\ &= (-1)^n\mathrm{Pf}[\mathcal{D}(k_x)\tau^x]. \end{aligned} \quad \text{(A13)}$$

The product inside the Pfaffian reads

$$\begin{aligned}\mathcal{D}(k_x)\tau^x &= \begin{pmatrix} E(k_x) & i\Delta U^\dagger\sigma^y U^* \\ -i\Delta U^T\sigma^y U & -E(k_x)\end{pmatrix}\begin{pmatrix} 0 & \mathbb{1} \\ \mathbb{1} & 0\end{pmatrix} \\ &= \begin{pmatrix} i\Delta U^\dagger\sigma^y U^* & E(k_x) \\ -E(k_x) & -i\Delta U^T\sigma^y U\end{pmatrix}, \end{aligned} \quad \text{(A14)}$$

where $E(k_x)$ is a diagonal matrix with entries given by $\{\varepsilon_\lambda + \lambda V + \varepsilon_0 - \mu \mp 2t\}$, $\lambda = \pm 1$. This matrix is indeed antisymmetric. One can easily see that, upon a reordering of the rows and columns described by a real unitary matrix $\mathcal{V}$, the matrix $\mathcal{D}(k_x)\tau^x$ can be put into a block diagonal form, where each block is a 4×4 matrix involving the particle states with eigenvalues differing only by the sign of V and their hole counterparts. Namely, each block has the form

$$\begin{pmatrix} 0 & -\Delta & \varepsilon + V & 0 \\ \Delta & 0 & 0 & \varepsilon - V \\ -\varepsilon - V & 0 & 0 & \Delta \\ 0 & -\varepsilon + V & -\Delta & 0\end{pmatrix}, \quad \text{(A15)}$$

where $\varepsilon = \varepsilon_\lambda + \varepsilon_0 - \mu \mp 2t$. Thus, this means that

$$\begin{aligned}&\mathrm{Pf}[\mathcal{H}_{\rm BdG}(k_x)\sigma^y\tau^y] \\ &= (-1)^n\mathrm{Pf}[\mathcal{D}(k_x)\tau^x] \\ &= (-1)^n\det(\mathcal{V})\prod_\lambda[V^2 - \Delta^2 - (\mu - \varepsilon_\lambda - \varepsilon_0 \pm 2t)^2], \end{aligned} \quad \text{(A16)}$$

where the upper and lower signs refer to $k_x = 0$ and $k_x = \pi/a$, respectively, and the matrix $\mathcal{V}$ is the same for both $k_x = 0, \pi/a$. Thus, we finally have

$$\begin{aligned}\mathcal{Q} &= \mathrm{sgn}\{\mathrm{Pf}[\mathcal{H}_{\rm BdG}(0)\sigma^y\tau^y]\mathrm{Pf}[\mathcal{H}_{\rm BdG}(\pi/a)\sigma^y\tau^y]\} \\ &= \prod_{\lambda,\eta=\pm 1}\mathrm{sgn}[\Delta^2 + (\mu - \varepsilon_\lambda - \varepsilon_0 + \eta 2t)^2 - V^2] \end{aligned} \quad \text{(A17)}$$

and consequently the phase boundaries are given by Eq. (8). We finally mention that analogous results have been found in Ref. 42 in the case of spinless fermions in a p-wave superconducting nanowire.

APPENDIX B: TRANSPORT ACROSS A NS JUNCYION

In this Appendix we investigate another important tool to assess the topological phase of an S-nanowire coupled to a normal electrode: the low-bias conductance across a NS junction in the tunneling limit. In the limit of low bias, transmission through the superconductor is completely suppressed and the conductance of the NS junction can be expressed in terms of the Andreev reflection matrix r_{he} (at the chemical potential)

$$G = \frac{2e^2}{h}\mathrm{Tr}[r^\dagger_{he}r_{he}] = \frac{2e^2}{h}\sum_{m=1}^{N_{\rm oc}} R_m. \quad \text{(B1)}$$

Here R_m are the eigenvalues of the Hermitian matrix $r^\dagger_{he}r_{he}$ and $N_{\rm oc}$ is the number of open channels in the normal electrode. Owing to particle-hole symmetry, the R_m's are either twofold degenerate or equal to 0 or 1.[33,43] The presence of a fully Andreev-reflected mode (giving a quantized contribution to the conductance) is a signature of the existence of an uncoupled Majorana fermion at the Fermi energy.[31,32] As a consequence, it is possible to write the conductance in the following form:[33]

$$G = \frac{2e^2}{h}\left(1 - \mathcal{Q} + 4{\sum_m}' R_m\right), \quad \text{(B2)}$$

where the primed sum is restricted to the degenerate Andreev reflection eigenvalues and $\mathcal{Q}$ is the topological invariant in Eq. (7). In the limit of poorly transparent barriers ($\gamma \ll 1$), we expect that almost all modes are fully reflected ($R_m \approx 0$, though never exactly zero)[33,43] and thus

$$G \approx \frac{2e^2}{h}(1 - \mathcal{Q}). \quad \text{(B3)}$$

As a consequence the low-bias conductance of the NS junction in the tunneling limit gives an important information on the topological phase of the S-nanowire.[29,31,32] This result can be extended to almost transparent barriers if we include a ballistic quantum point contact close to the NS interface.[33] In Fig. 12 we show the conductance G (in units of $2e^2/h$) as a function the parameter γ controlling the transparency of the barrier. In the tunneling limit ($\gamma \ll 1$), we notice that the conductance approaches 0 for a topologically trivial S-nanowire (red dashed line, $V/t = 0.2$ and $\mu/t = 1.5$) or $2e^2/h$ for a topologically nontrivial S-nanowire (blue solid line, $V/t = 0.2$ and $\mu/t = 1.1$), in agreement with Eq. (B3).

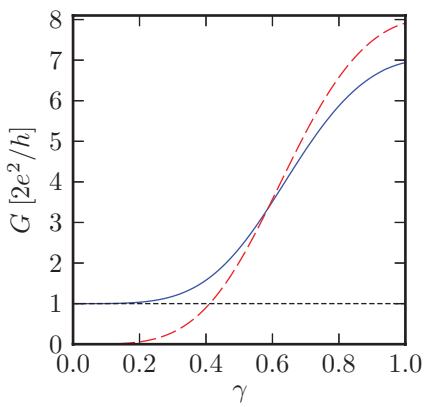

FIG. 12. (Color online) Conductance (in units of $2e^2/h$) of the NS junction as a function of the parameter γ controlling the transparency of the barrier. The (blue) solid line refers to a S-nanowire in the topologically nontrivial phase ($V/t = 0.2$ and $\mu/t = 1.1$), while the (red) dashed line refers to a S-nanowire in the topologically trivial phase ($V/t = 0.2$ and $\mu/t = 1.5$).

*marco.gibertini@sns.it
†http://qti.sns.it/

[1] E. Majorana, Nuovo Cimento **14**, 171 (1937).
[2] F. Wilczek, Nat. Phys. **5**, 614 (2009).
[3] C. W. J. Beenakker, e-print arXiv:1112.1950.
[4] J. Alicea, e-print arXiv:1202.1293.
[5] G. Moore and N. Read, Nucl. Phys. B **360**, 362 (1991).
[6] N. Read and D. Green, Phys. Rev. B **61**, 10267 (2000).
[7] D. A. Ivanov, Phys. Rev. Lett. **86**, 268 (2001).
[8] L. Fu and C. L. Kane, Phys. Rev. Lett. **100**, 096407 (2008).
[9] A. Y. Kitaev, Phys.-Usp. **44**, 131 (2001).
[10] J. D. Sau, R. M. Lutchyn, S. Tewari, and S. Das Sarma, Phys. Rev. Lett. **104**, 040502 (2010).
[11] J. Alicea, Phys. Rev. B **81**, 125318 (2010).
[12] J. D. Sau, S. Tewari, R. M. Lutchyn, T. D. Stanescu, and S. Das Sarma, Phys. Rev. B **82**, 214509 (2010).
[13] R. M. Lutchyn, J. D. Sau, and S. Das Sarma, Phys. Rev. Lett. **105**, 077001 (2010).
[14] Y. Oreg, G. Refael, and F. von Oppen, Phys. Rev. Lett. **105**, 177002 (2010).
[15] C. Nayak, S. H. Simon, A. Stern, M. Freedman, and S. Das Sarma, Rev. Mod. Phys. **80**, 1083 (2008).
[16] M. Sato, Y. Takahashi, and S. Fujimoto, Phys. Rev. B **82**, 134521 (2010).
[17] A. C. Potter and P. A. Lee, Phys. Rev. B **83**, 094525 (2011).
[18] T. Stanescu, R. M. Lutchyn, and S. Das Sarma, Phys. Rev. B **84**, 144522 (2011).
[19] J. D. Sau, C. H. Lin, H.-Y. Hui, and S. Das Sarma, Phys. Rev. Lett. **108**, 067001 (2012).
[20] A. R. Akhmerov, J. P. Dahlhaus, F. Hassler, M. Wimmer, and C. W. J. Beenakker, Phys. Rev. Lett. **106**, 057001 (2011).
[21] A simple relation between the transmissivity $\mathcal{T}$ of the barrier and the parameter γ cannot be, in general, derived. We simply notice that in the tunneling limit ($\gamma \ll 1$) we expect that $\mathcal{T} \propto \gamma^2$.
[22] P. G. de Gennes, *Superconductivity of Metals and Alloys* (Benjamin, New York, 1966).
[23] P. Ghosh, J. D. Sau, S. Tewari, and S. Das Sarma, Phys. Rev. B **82**, 184525 (2010).
[24] M. Wimmer, e-print arXiv:1102.3440.
[25] J. Tersoff and D. R. Hamann, Phys. Rev. B **31**, 805 (1985).
[26] C. J. Chen, *Introduction to Scanning Tunneling Microscopy* (Oxford University Press, Oxford, 1993).
[27] S. Sanvito, C. J. Lambert, J. H. Jefferson, and A. M. Bratkovsky, Phys. Rev. B **59**, 11936 (1999).
[28] G. Kells, D. Meidan, and P. W. Brouwer, Phys. Rev. B **85**, 060507(R) (2012).
[29] K. Sengupta, I. Žutić, H.-J. Kwon, V. M. Yakovenko, and S. Das Sarma, Phys. Rev. B **63**, 144531 (2001).
[30] Similar broadening effects have been observed also in metal-topological insulator junctions; J. A. Hutasoit and T. D. Stanescu, Phys. Rev. B **84**, 085103 (2011).
[31] K. T. Law, P. A. Lee, and T. K. Ng, Phys. Rev. Lett. **103**, 237001 (2009).
[32] Karsten Flensberg, Phys. Rev. B **82**, 180516 (2010).
[33] M. Wimmer, A. R. Akhmerov, J. P. Dahlhaus, and C. W. J. Beenakker, New J. Phys. **13**, 053016 (2011).
[34] For a recent study of different types of topological phase transitions in two-dimensional topological superconductors, see Phys. Rev. Lett. **108**, 087003 (2012).
[35] S. Tewari, J. D. Sau, V. W. Scarola, C. Zhang, and S. Das Sarma, Phys. Rev. B **85**, 155302 (2012).
[36] A. M. Black-Schaffer and J. Linder, Phys. Rev. B **84**, 180509(R) (2011).
[37] L. Fu and C. L. Kane, Phys. Rev. B **79**, 161408 (2009).
[38] H.-J. Kwon, V. M. Yakovenko, and K. Sengupta, Low Temp. Phys. **30**, 613 (2004).
[39] To be more precise, the superconducting pairing induced in a one-dimensional wire with SO coupling is purely of the type $(p_x + ip_y)$ only if the chirality component of the dispersion curve with higher energy can be neglected. This happens when $V \gg \Delta$. Moreover, an increase of the Zeeman field produces a decrease of the effective gap E_g, reinforcing the validity of the Andreev approximation.
[40] C. W. J. Beenakker, Phys. Rev. Lett. **67**, 3836 (1991).
[41] K. T. Law and P. A. Lee, Phys. Rev. B **84**, 081304 (2011).
[42] Bin Zhou and Shun-Qing Shen, Phys. Rev. B **84**, 054532 (2011).
[43] B. Béri, Phys. Rev. B **79**, 245315 (2009).